

Article

Factorial Mixture Design for Properties Optimization and Modeling of Concrete Composites Incorporated with Acetates as Admixtures

Ammar Ali Abed ^{1,2,*}, Alireza Mojtahedi ² and Mohammad Ali Lotfollahi Yaghin ²¹ Department of Engineering Affairs, General Company for Ports of Iraq, Basrah 61004, Iraq² Department of Water Resources Engineering, Faculty of Civil Engineering, University of Tabriz, Tabriz 51368, Iran; a.mojtahedi@tabrizu.ac.ir (A.M.); lotfollahi@tabrizu.ac.ir (M.A.L.Y.)

* Correspondence: eng.ammar@tabrizu.ac.ir

Abstract: Nowadays, admixtures are used with the aim to provide strength and durability to concrete with less water use. New and low-cost admixtures gained a large amount of consideration to mitigate the problems associated with concrete's durability and service life without upsetting its strength properties. The current work investigates the effect of three types of acetates on the workability, density, and compressive strength of concrete, which is used in structures of the Iraqi ports that suffer from corrosion damages and deterioration owing to the aggressive marine environments. Potassium acetate (KA), calcium acetate (CaA), and ethyl acetate (EA) are incorporated with different doses (1.38–5.6 wt.% of cement) in concrete mixtures using different water/cement ratios (0.48–0.54) based on an espoused central composite experimental design. The experimental results confirmed that the average workability increased with increasing the acetate dose, particularly with CaA. The density and compressive strength of 28 days of water-cured mixtures increased with increasing acetate dose following the order: Ca > K > Ethyl acetate and decreased with increasing w/c ratio. The high rise in compressive strength and workability linked to control mixtures was 30.8% and 77.3% as well as 15.7% and 64.3% for the mixtures incorporated with 5.6 wt.% CaA and KA, respectively. While it was 14.2% and 58.3% for the mixtures incorporated with 3.5 wt.% EA. RSM was employed to optimize and model the design and hardened properties of concrete mixtures. ANOVA results predicted the same trend, which was obtained from the experimental results. The mathematical models were valued with high-regression coefficients. The highest compressive strength of 42.68 MPa has been achieved for a concrete mixture of 0.48 w/c ratio by the incorporation of 5.1 wt.% CaA through a model with R² 96.97%. The relatively low-cost acetate admixtures, particularly CaA, seemed promising for the fabrication of concrete with outstanding properties.



Citation: Abed, A.A.; Mojtahedi, A.; Lotfollahi Yaghin, M.A. Factorial Mixture Design for Properties Optimization and Modeling of Concrete Composites Incorporated with Acetates as Admixtures. *Sustainability* **2023**, *15*, 10608. <https://doi.org/10.3390/su151310608>

Academic Editor: Ramadhansyah Putra Jaya

Received: 19 May 2023

Revised: 1 July 2023

Accepted: 3 July 2023

Published: 5 July 2023



Copyright: © 2023 by the authors. Licensee MDPI, Basel, Switzerland. This article is an open access article distributed under the terms and conditions of the Creative Commons Attribution (CC BY) license (<https://creativecommons.org/licenses/by/4.0/>).

Keywords: acetates; compressive strength; concrete; optimization; response surface methodology; workability

1. Introduction

Iraq owns many commercial ports with distinguished rural locations. They occupy an effective position in the national economy. The ports are designated for commercial purposes (import and export). They are located in the Basra governorate, on the right bank of the Shatt al-Arab, such as the port of Al-Maqil, Abu Flus, Umm Qasr, and Khor al-Zubayr. Although the Iraqi ports have an important geographical location in world trade, as they are considered the ideal way for transit traffic trade between East and Southeast Asia and Europe, the ports have suffered many challenges including environmental stresses, resulting in corrosion damages and deterioration of the structures of the ports exposed to the aggressive marine environments, in particular, the high salinity of seawater with an average of about 40.5 g/kg [1]. Therefore, it became essential and economical to plan port activities in order to reduce port activity disruption by preserving port infrastructure,

rather than demolishing and reconstructing the damaged facilities. This can be practiced by applying some concrete corrosion mitigation procedures using anti-corrosion materials as concrete admixtures.

It is well-confirmed that materials are one of the most important considerations for solving the shortcoming in concrete. In severe exposure conditions, the specification and/or use of unsuitable materials can lead to poor durability; therefore, using efficient materials in construction has become the most innovative method used for construction projects. In addition, using low water-to-cementitious materials ratio and supplementary materials will provide denser and more durable concrete equated with representative Portland cement concrete [2].

Several additives have been applied to obtain low permeability, high density, and load-carrying capacity, as well as consent for the building of durable and high-strength concrete structures. Among those additives are nanoparticles including nano-silica (nano-SiO₂), nano-alumina (nano-Al₂O₃), nano-ferric oxide (nano-Fe₂O₃), nano-titanium oxide (nano-TiO₂), carbon nanotubes (CNTs), graphene and graphene oxide [2–4]. Moreover, nanopolymers were found to participate in self-healing mechanisms [5,6], as well as rewarding an improved product layer on the steel surface and calcium content in the bulk matrix [7].

Among other additives are corrosion inhibitors which are added in slight amounts to extend the corrosion start time and avoid the onset of corrosion in reinforced concrete structures [8]. These include inorganic inhibitors, such as nitrates, chromates, molybdate, phosphate, carbonates, polyphosphates, and silicates [9–13], as well as organic inhibitors including amines and alkanol amines and their salts. The organic inhibitors can inhibit steel corrosion through an adsorption mechanism by forming a thin layer of shielding barrier film on the surface of the rebar [11,14]. Moreover, corrosion inhibitors may be embedded in microcapsules that could be added into fractured concrete and successfully passivated or maintained the inactiveness of the rebar when the concrete is damaged [15]. However, controlling the concrete, such as using low w/c ratios, increasing cement content in the concrete composition, and optimizing the inhibitor dose leads to better anticorrosion resistance [16].

In addition, the growth and operative application of chemical admixtures in concrete technology resulted in new advancements in the formulation and application of cement and concrete composites. The incorporation of a small amount of admixture could effectively adjust the performance of cement-based materials. The improvement includes the physical, mechanical, durability, rheology, and hydration properties [17]. The functional groups of admixtures are generally categorized into hydroxyl, carboxyl, amino, and sulfonic acid [18]. However, it was pointed out that modifying and improving the performance of hydroxyl- or carboxyl-containing admixtures could be carried out by esterification [19].

Superplasticizers are one of the admixtures that act to modify the concrete workability, and at the same time, increase the strength of concrete. They neutralize the surface attractions between cement particles resulting in a less open structure that requires less water/cement ratio; therefore, increasing the strength and durability of concrete. However, most of the superplasticizers used are synthetic and more expensive than other types of concrete admixtures [20].

On the other hand, new green and low-cost admixtures that can work efficiently in the presence of water are developed by some researchers. Those additives are added to mitigate the problems associated with concrete's durability and service life without upsetting its strength properties [21,22].

From a different perspective, RSM is an efficient statistical tool that has been widely used and successfully employed to set the experimental design and models that mathematically describe the effects of the operating parameters on the process's responses. Literature information on using RSM in the optimization and modeling of concrete mixture design and properties is highlighted in the methodology and results in parts of the current work.

There are limited studies regarding increasing the durability of concrete by incorporating acetates as an admixture. The literature studies are concentrated on using sodium acetate (CH_3COONa) [23–27]. However, the studies lack investigation and optimization of the effect of other types of metal acetates and organic acetates on the strength and physical characteristics of cementitious materials.

The objectives of the current work are to pave the way for the application of acetates as admixtures in the construction of Basrah port infrastructure by providing scientific knowledge about the standardized procedures used to fabricate and test the properties of reinforced concrete specimens incorporated with diverse kinds of acetates, as well as to determine the optimum features of acetates to achieve high strength and durability properties. The current part of the work focuses on using potassium acetate, calcium acetate as inorganic acetates, and ethyl acetate as organic acetate in unreinforced concrete. The research studies the effect of acetate type and amount, and the water-to-cement ratio on workability, density, and compressive strength. The effect of the variables is optimized and modeled using a two-factorial central composite experimental design.

2. The Experimental Part

2.1. Materials

Ordinary Portland cement (OPC) confirming Iraqi specifications (Iraqi standards 2019) [28], natural sand passing through a 2.36 mm sieve, gravel passing through a 20 mm sieve, and tap water were used as concrete main ingredients. Potassium acetate (KA), calcium acetate (CaA), and ethyl acetate (EA) with an assay of $\geq 99\%$ are purchased from Fluka™ Chemicals and Reagents for Analytical Chemistry and used as admixtures. The mixture proportions (1:2:4) for concrete were used. Fresh concrete mixtures were prepared using 90% of the total amount of water needed for the concrete mix. The remaining amount of water was used to dissolve the predetermined amount of the acetate. The acetate solution was added to the fresh concrete mixture. All samples were mixed in a laboratory drum mixer. Concrete mixtures incorporated with different types (Ka, CaA, and EA) and doses (1.38–5.6 wt.%) in concrete mixtures using different water/cement ratios (0.48–0.54) based on an espoused central composite experimental design were formulated, molded, and cured in water at room temperature for 28 days and then tested. Three samples were formulated for each test taking into account the average value. Control samples without acetates were formulated, molded, cured, and tested similarly for comparison purposes. Figure 1 shows images of some aspects of the experimental work.



Figure 1. (a) Slump test, (b) mold preparation, (c) a typical casted specimen, (d) cured specimens.

2.2. Methodology

Response surface methodology (RSM) is a powerful methodology that uses statistical techniques based on the partial factorial design that is employed to optimize and model specific responses influenced by the process operating variables. The attractive feature of

RSM made the tool popular and has significant potential [14,29,30]. The importance of RSM could be summarized by its applications in various processes for designing simultaneous runs, which could be performed quickly ensuring savings in the process time, expense, and effort. In the current work, mathematical and statistical software was used as a tool to identify the relationships between the type and content of the acetate additives and the water/cement ratio of the concrete mixtures as independent operating parameters on workability, density, and compressive strength as dependent variables (responses), and to optimize and establish the mathematical models that describe the mentioned relations. The methodology used is carried out by using appropriate design and analysis of experiments in an empirical way based on a two-factorial central composite design followed by the response surface methodology.

The individual and interactive effects of the content of the acetates and water/cement ratio on the responses were studied through 10 experimental runs. The mathematical empirical model is fitted to evaluate the impact of each independent operating parameter on the responses. The empirical model is demarcated as:

$$Y = \beta_0 + \beta_1X_1 + \beta_2X_2 + \beta_{11}X_1^2 + \beta_{22}X_2^2 + \beta_{12}X_1X_2 \quad (1)$$

The response (Y) is correlated to the set of regression coefficients (β): The model intercept is (β_0); β_1 and β_2 are linear terms; β_{12} is the interaction term; β_{11} and β_{22} are quadratic coefficient terms. The software portable statgraphics centurion 15.2.11.0.exe was used for the regression and graphical analysis of data.

The three types of acetates were incorporated with different doses (1.38–5.6 wt.%) in concrete mixtures using different water/cement ratios (0.48–0.54) based on the adopted central composite experimental design. Table 1 shows the experimental design with the actual operating parameter levels and the response values.

Table 1. The adopted experimental design includes the actual levels of the operating parameters as well as the average values of the responses.

The Operating variables		Exp. No.								
		1	2 *	3	4	5	6	7	8	9
(Acetate/cement) % wt.		3.50	3.50	2.00	5.00	2.00	5.60	5.00	1.38	3.50
W/C		0.48	0.51	0.49	0.49	0.53	0.51	0.53	0.51	0.54
Type of acetate	Concrete Property	Exp. No.								
		1	2 *	3	4	5	6	7	8	9
K acetate	Compressive strength (MPa)	38.90	32.45	35.80	37.00	25.29	33.61	29.12	29.80	25.02
	Density (g/cm ³)	2.39	2.37	2.37	2.41	2.38	2.408	2.376	2.393	2.365
	Slump (cm)	2.00	4.00	3.50	4.50	2.00	3.00	4.50	2.00	5.00
Ca acetate	Compressive strength (MPa)	42.88	40.50	39.98	41.97	35.82	40.89	37.22	38.31	33.60
	Density (g/cm ³)	2.39	2.37	2.37	2.40	2.37	2.385	2.38	2.36	2.37
	Slump (cm)	3.0	3.5	7.0	10.0	15.0	18.0	8.0	4.0	6.0
Ethyl acetate	Compressive strength (MPa)	35.20	33.9	32.10	29.70	27.29	26.10	32.90	28.99	27.30
	Density (g/cm ³)	2.43	2.37	2.42	2.43	2.39	2.397	2.405	2.393	2.399
	Slump (cm)	2.50	3.00	5.00	3.00	5.00	3.50	5.00	4.00	4.50
(Without acetate)	Compressive strength (MPa)	29.36		29.36		28.31		25.96		24.88

* Repetitions.

2.3. The Properties Investigated

The workability of fresh concrete mixtures is the measure of the ease with which the concrete composites flow and consolidate. Workability is a critical factor that affects the long-term performance of hardened concrete, which may complicate the compaction of

cement composites due to the trapping of air spaces that highly affects the mechanical performance [31].

Standard flow tests for measuring the workability were conducted immediately after mixing freshly mixed concrete composites using a slump cone. The cone was filled in three layers and manually tamped 25 times. After filling all the layers and cleaning around the slump cone, the slump cone was removed within 3 to 5 s in a straight ascending direction. Slump reading is the difference in height of the slump cone and average of the height of the concrete specimen. The average of four measurements represented the test findings.

Dried concrete cubes of $150 \times 150 \times 150$ mm that are cured purely in water for 28 days were tested for density. The volume of the cubes was accurately measured after weighing the cubes. The density of the concrete specimens was obtained as the average of the three test results.

A compressive strength machine control model 50-C23C02 with a 2000 KN load capacity was used to test the compressive strength of $150 \times 150 \times 150$ mm concrete cubes. The load was applied at a constant rate until the specimen failed. The compressive strength of concrete was obtained as the record of the failure load. The average of the three test results represented the average compressive strength.

3. Results and Discussion

3.1. The Experimental Results

Compressive strength is the main property that affects the fundamental behavior of construction elements. The experimental findings concerning the average values of compressive strength of concrete mixtures cured for 28 days are shown in Figure 2. The mixtures were formulated with different w/c ratios and incorporated with different types and doses of acetates. The results confirmed that the compressive strength of concrete could be increased by the incorporation of the three acetates of admixtures compared to the control samples; however, the mixtures incorporated with calcium acetate seemed to exhibit the highest compressive strength followed by the mixtures with potassium acetate than ethyl acetate. In general, the compressive strength increases with increasing the dose of the three types of acetate; however, concrete mixtures incorporated with ethyl acetate exhibited maximum compressive strength at a content of 3.5% (Figure 2).

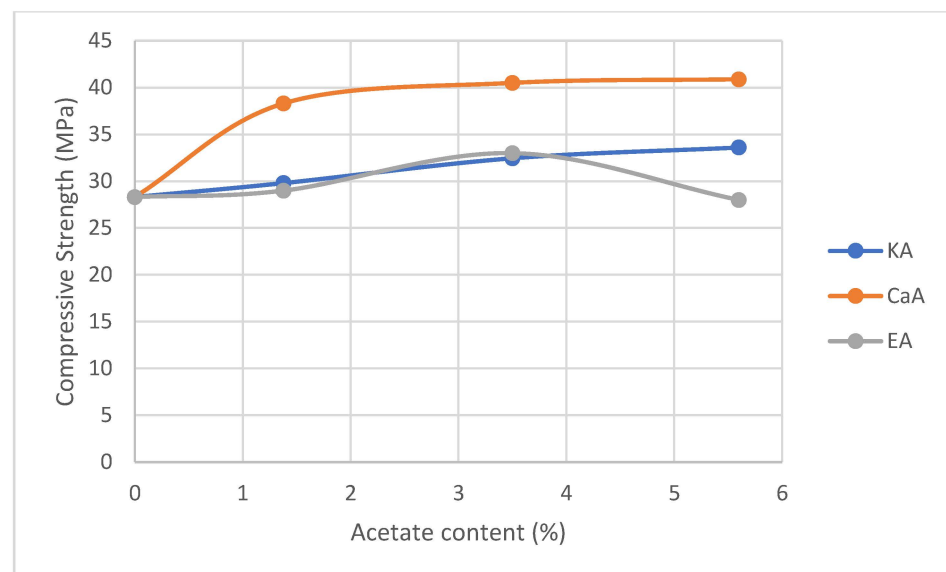


Figure 2. Compared to control specimens, the variation of compressive strength with acetates content for mixtures of (w/c = 0.51).

In general, the interaction between cement and admixtures is a surface phenomenon. Some evidence of chemical interactions between the cementitious phase and acetates was

acknowledged and documented [18,32,33]. Acetates, such as KA, CaA, and EA that are used in the current work undergo hydrolysis when dispersed in an alkaline medium. The alkaline medium in the cement pastes is the $\text{Ca}(\text{OH})_2$ -saturated pore solution. The dissolution of cement grains leads to the release of Ca^{+2} . The alkaline hydrolysis of the acetate admixture leads to the release of acetate anion CH_3COO^- . The combination of the calcium and acetate ions resulted in the formation of the organic salt (calcium acetate). Figure 3 shows a scheme of the interactions described above.

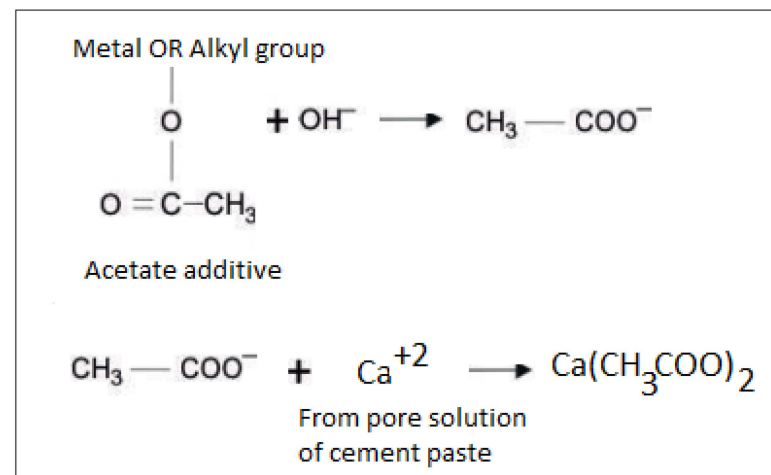


Figure 3. Scheme of the interactions of acetate admixtures with cement.

The chemical interaction could result in changes in the morphology and composition of the hydrated cement phases and increase the amounts of the hydrates which enhance the strength of the dried mixtures.

It indicated that the order of increasing the compressive strength of concrete mixtures was incorporated with $\text{Ca} > \text{K} > \text{Ethyl acetate}$. The situation may be attributed to the size of the acetate partner (Ca, K metal atoms, and the organic ethyl group) and its chemical nature, which are the factors that may play an important role in boosting the compressive strength. Regarding the size of the acetate partner, the smaller the size of the acetate partner, the more the enhancement in the tendency of linkages that lead to a more compacted concrete morphology. The small size of the calcium atom (Ca^{+2} radius = 114 pm) was compared to the K atom (K^{+1} radius = 152 pm) [34], and the larger size of ethyl group may be behind the aforementioned order of compressive strength of the mixtures which are formulated in the current study. Concerning the nature of the acetate partner, the stronger chemical bonding of the inorganic Ca and K metal ions with cement ingredients compared to the weaker physical linkages of the organic ethyl group is also one of the causes behind the higher compressive strength values of the mixtures incorporated with Ca and K acetates. The supreme increase in compressive strength linked to conventional mixtures was 30.8% and 15.7% for the mixtures incorporated with 5.6% CaA and KA, respectively. While it was 14.2% for the mixtures incorporated with 3.5% ethyl acetate.

The findings of the experimental work for the variation of compressive strength of concrete with w/c ratio revealed that strength rises with the declining w/c ratio using the three types of acetates. A typical illustration showing the tendency of decreasing the compressive strength of concrete mixtures using similar acetate content (3.5%) with the increasing w/c ratio is clarified in Figure 4.

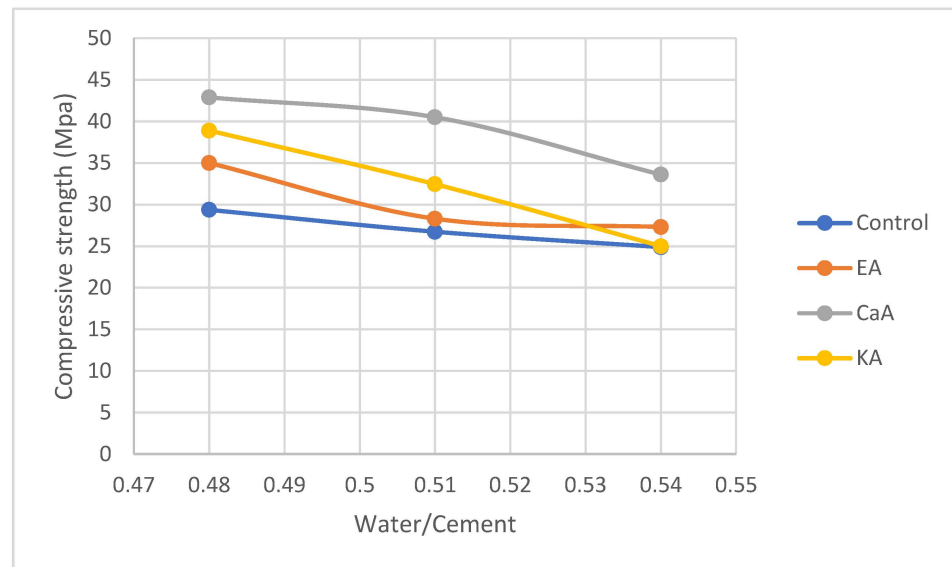


Figure 4. Compressive strength set against w/c ratio for concrete mixtures incorporated with 3.5% cement weight of the acetates.

A high w/c ratio causes aggregate segregation from the cement paste. Moreover, not consuming water by the hydration reaction may lead to microscopic pores (bleeding) and shrinkage resulting in declining the concrete strength.

Figure 5 shows the average workability results for the fresh concrete mixtures of w/c ratio of 0.51 containing different types and contents of acetates. It is noticed that increasing the content of acetates in the concrete mixtures augments its consistency. Notable compacted composites with no observable cracks were obtained.

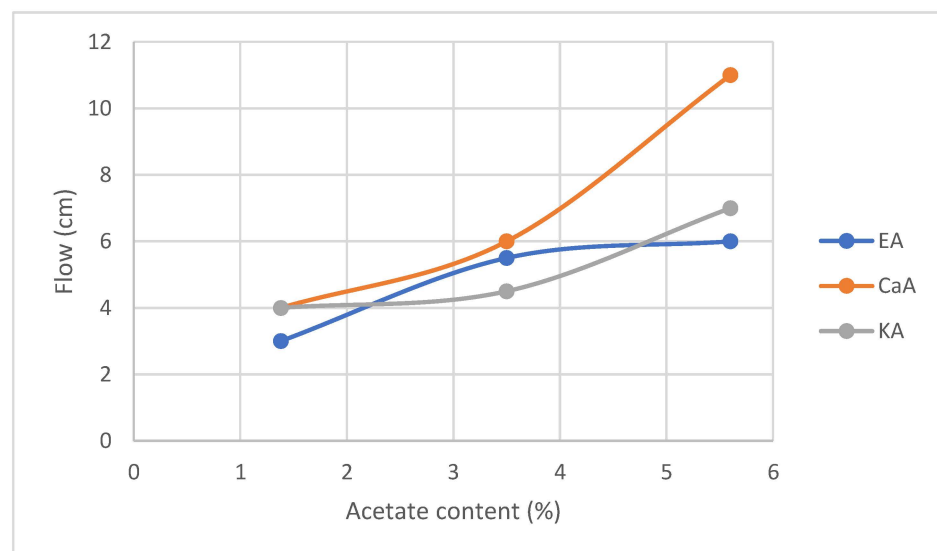


Figure 5. Average workability versus acetate content in concrete mixtures (w/c = 0.51) incorporated with different acetates.

The increase in workability is more announced for the mixtures incorporated with the metallic calcium and potassium acetates. The reason may be attributed to the fact that when the acetates dissociate in water, CH_3COO^- ions form. The metal ions already present in the cement, such as Na^+ and Ca^{+2} will react with the acetate ions. The product of this reaction comprises crystals of metal acetate. The dissociated K^+ and Ca^{+2} ions will react with free water and produce KOH and $\text{Ca}(\text{OH})_2$. Moreover, acetic acid (CH_3COOH) is

produced by the reaction of free water with CH_3COO^- ions. Suppose a large quantity of acetate admixture is added to the mixture. In that case, the formation of acetic acid in the mixture may delay the hydration process and increase the workability of the concrete mixtures. Similar findings were reported in [25]. The result of the dissociation of ethyl acetate also produces acetic acid that contributes to delaying the hydration reaction as well as increasing the mixture's workability.

The experimental results for the slump shown in Table 1 revealed that at a w/c ratio of up to 0.51, the increase in the calcium acetate content resulted in an increase in the slump. Moreover, the situation may be attributed to the adsorption of the hydrolyzed Ca ions from CaA on the surface of the cement particles owing to the concentration incline of Ca ions between the cement particles and liquid, in order that the cement particles become well dispersed due to mutual repulsion, causing the increase in slump. However, at a high w/c ratio (0.53 for experiment Nos. 5 and 7) the results revealed that increasing calcium acetate content (from 2% to 5%) gave rise to the decrease in slump. The decrease in slump may be attributed to the interaction effect of the two variables. The dilution effect of the high-water content may cause the desorption of Ca ions from the surface of cement particles leading to less-dispersed cement particles. Lowering the dispersity of the cement particles leads to a decrease in the slump values (workability). Therefore, it can be deduced that both the acetate content and w/c ratio govern the hydration process.

3.2. ANOVA Results

Analysis of variance (ANOVA) results for compressive strength are illustrated in Figures 6–8. The results confirmed that the acetate type, acetate amount, and w/c ratio remarkably affect compressive strength. The findings are reflected in the plots resulting from the analysis of the experimental compressive strength results by the RSM software. Pareto charts which show the absolute values of the properties show that the impact of the two operating parameters on compressive strength is significant (the effects extend past the reference line). However, the effect of the acetate content is more significant for EA (Figure 8a), while for CaA and KA, the w/c ratio seemed more significant (Figures 6a and 7a). The situation may be related to the chemical nature of the acetates. Ka and CaA are mineral acetates that have a good affinity to water, while EA is a non-metallic acetate that has an organic part of poor affinity to water. The mean effect plots indicated that compressive strength is highly affected by the w/c ratio, which decreases with increasing w/c ratio, in particular at higher w/c ratios. A dramatic decrease was observed for the mixtures with KA and CaA (Figures 6b and 7b), while mixtures with EA showed a flat maximum (Figure 8b). The reason for growing the strength by increasing the acetate amount may be due to the reaction of calcium hydroxide present in concrete with K and Ca in water. The product of this reaction is silica gel that will grow into solid crystals that adhere to the walls of the pores after hydration giving the concrete rigidity and strength. However, the compressive strength rises with increasing the content of EA up to a maximum and then decreases (Figure 8b), while for CaA and KA, the mixture of compressive strength rises with increasing the acetate content in a closely linear mode (Figures 6b and 7b). Decreasing the compressive strength of the mixtures incorporated with EA after the maxima may be attributed to the fact that at higher concentrations of EA, the repulsion forces between the organic EA which has low solubility in water and the polar constituents of concrete mixture will increase, leading to more porous and less compacted concrete microstructure. In agreement with our findings, it was reported that adding acetate could increase the content of ettringite and portlandite in the concrete [35].

Furthermore, the interaction plots display the mean effect of acetate content versus the w/c ratio at each level. No interaction effects of the operating variables for compressive strength were observed for the mixtures incorporated with CaA and KA (Figures 6c and 7c). The situation is reflected by the parallel lines of the effects. While the interaction plots reflected remarkable interaction effects for the compressive strength of the mixtures incorporated with EA, in particular at a w/c ratio above 0.48 (Figure 8c). The situation

is visualized by the cross lines that suggest the interaction. The behavior above is more apparent throughout the contours shown in the two-dimensional (2D) plot (Figure 8g). The elliptical shapes of the contours indicate the variable's substantial interactions.

The normal probability plot presented in (Figures 6d, 7d and 8d) revealed the model's effectiveness by displaying the adjacent positions of the points to the straight lines. The three-dimensional (3D) response surface plots (Figures 6f, 7f and 8f) illustrate the conception of the response surface and the style of the compressive strength performance in terms of the two operating factors.

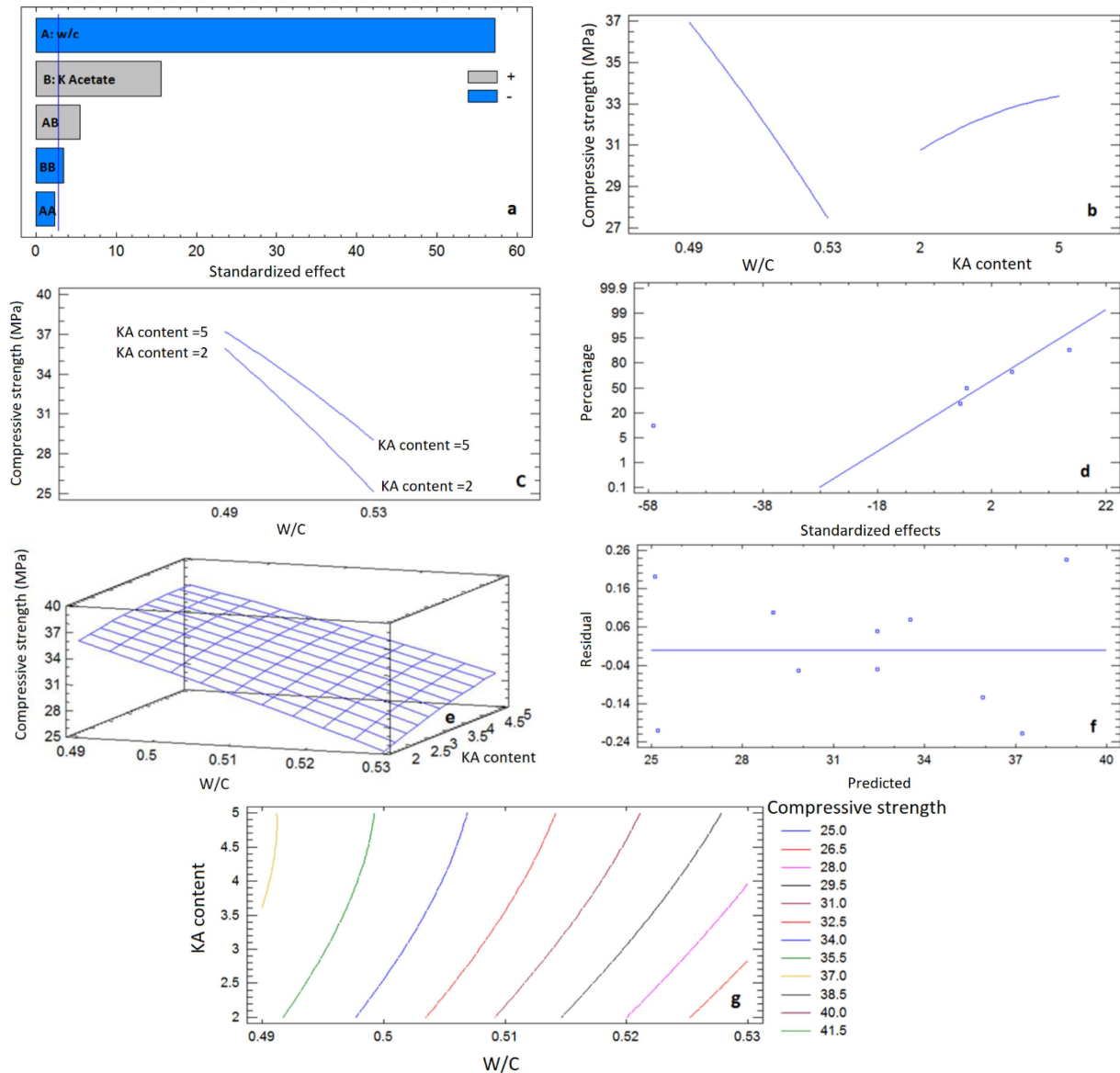


Figure 6. Plots of Pareto chart (a), main effects (b), interaction (c), normal probability (d), response surface (e), residual (f), and contour (g) for compressive strength of concrete mixtures incorporated with potassium acetate (KA).

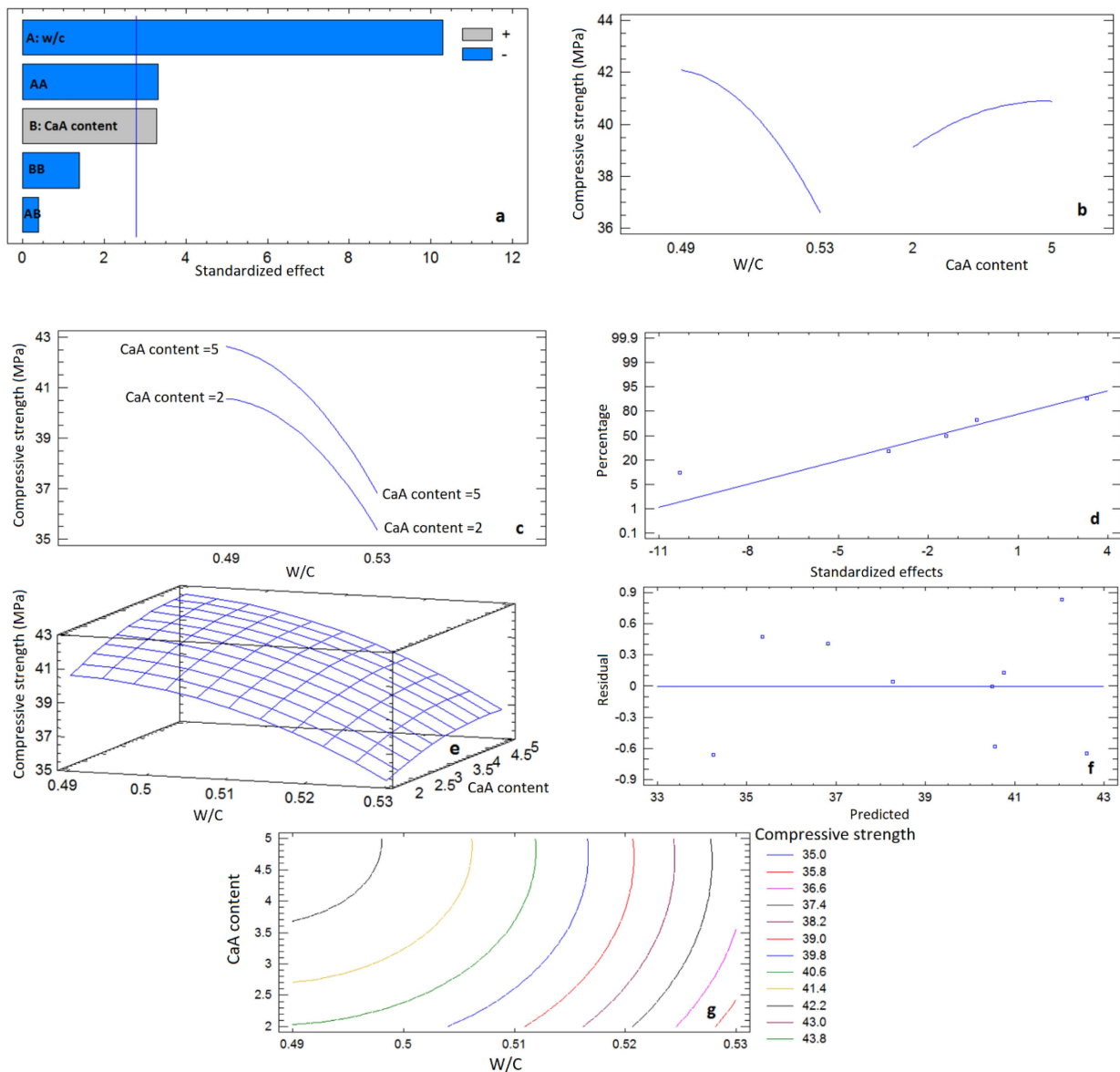


Figure 7. Plots of Pareto chart (a), main effects (b), interaction (c), normal probability (d), response surface (e), residual (f), and contour (g) for compressive strength of concrete mixtures incorporated with calcium acetate (CaA).

The contour plots show how varying the two operating variables affects the predicted compressive strength values, which are represented as colors. Figures 6g and 7g show the two-dimensional (2D) contour plots for KA and CaA mixture. The figures reflect less effective interactions between the variables. The non-elliptical shapes of the contours specify the situation.

The plots of the residuals (Figures 6e, 7e and 8e) verify the validity of the regression. The random scattering of residuals versus predicted reflects that the errors are independent. The fall of the points randomly on both sides of (0) demonstrates the normal distribution of the points. The results obtained affirm that the espoused model can be utilized to detect the optimum compressive strength and that it is appropriate for usage. The methodology was applied successfully to optimize and model the properties of concrete composites including compressive strength [36–39].

The empirical regression model equations, regression coefficients, and the optimum compressive strength values and operating variables for the mixtures formulated with

different acetates are listed in Table 2. The R^2 is reasonable for fitting uniformity. The high-regression coefficient proves that the estimated models are accurate and can explain the experimental results successfully.

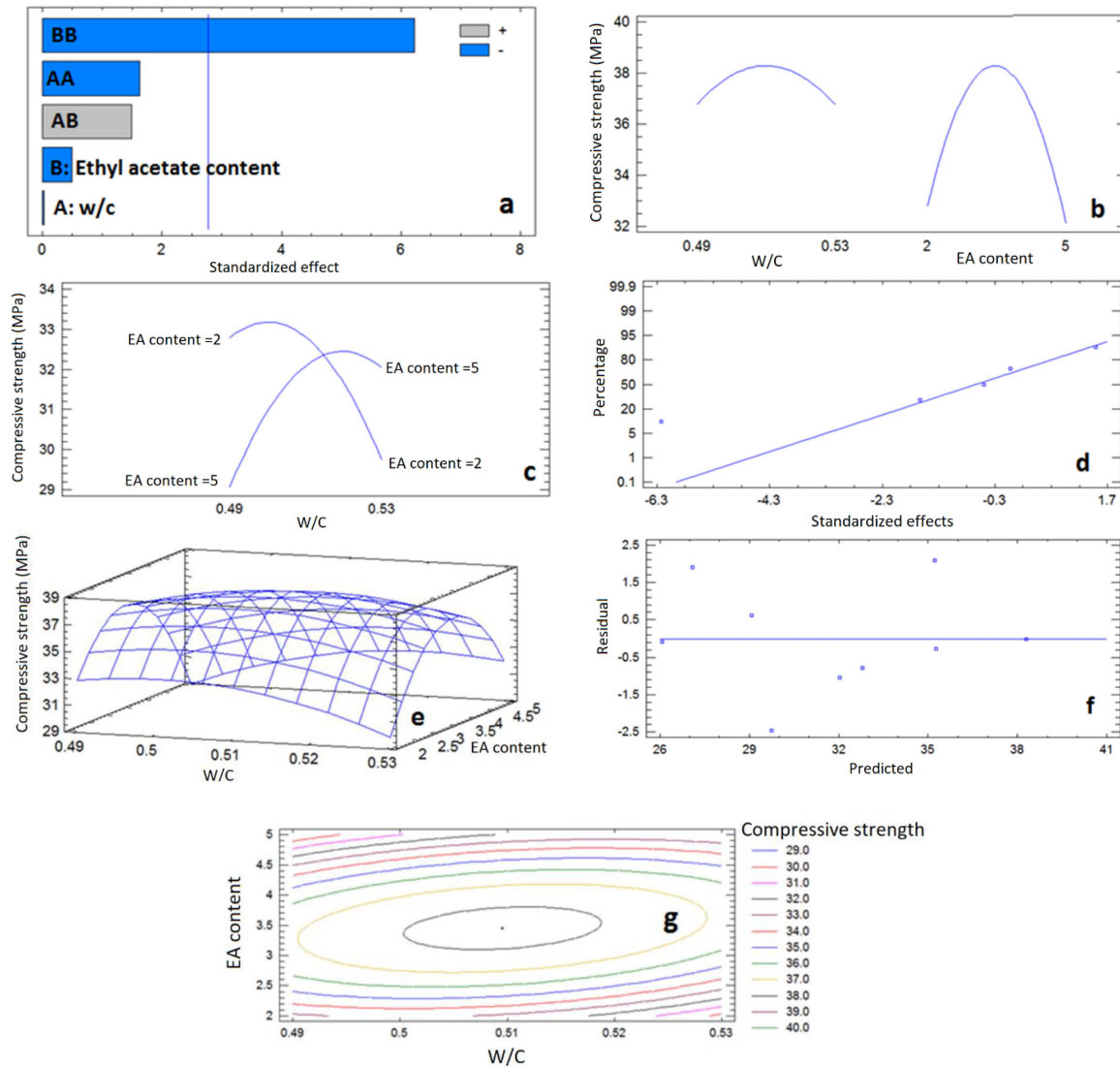


Figure 8. Plots of Pareto chart (a), main effects (b), interaction (c), normal probability (d), response surface (e), residual (f), and contour (g) for compressive strength of concrete mixtures incorporated with ethyl acetate (EA).

Table 2. The empirical regression model equations, regression coefficients, and the optimum compressive strength values and operating variables for the mixtures formulated with different acetates.

Acetate Type	The Generated Empirical Regression Model Equation	Regression Coefficient R^2 (%)	Optimized Compressive Strength Value (MPa)	Optimized Operating Variables
Ca	Compressive strength = $-665.62 + 2871.01 W + 4.63 A - 2932.86 W^2 - 4.92 W A - 0.22A^2$	96.97	42.68	w/c = 0.48 and CaA content = 5.1%
K	Compressive strength = $20.70 + 339.75 W - 8.99 A - 640.64 W^2 + 21.67 W K - 0.17 A^2$	99.89	38.76	w/c = 0.48 and KA content = 4.24%
Ethyl	Compressive strength = $-898.76 + 3728.86 W - 7.52 A - 3828.22 W^2 + 50.0 W A - 2.62 A^2$	91.41	38.31	w/c = 0.51 and EA content = 3.45%

Where W = W/C, A = acetate content (wt.%)

ANOVA results for bulk density confirmed that the acetate type, acetate content, and w/c ratio remarkably influence density. However, the effect of acetate content is more significant (Figures 9a, 10a and 11a). The mean effect plots indicated that density declines with the rising w/c ratio and increases with increasing the acetate amount, particularly at high-acetate contents (Figures 9b, 10b and 11b). The rise in density may be ascribed to the decrease in air in the cement matrix as acetates fill the empty spaces within the pore structure. The higher density values may be due to the improvement in the hydration process and subsequently the increase in the hydration products was compared with those of control samples.

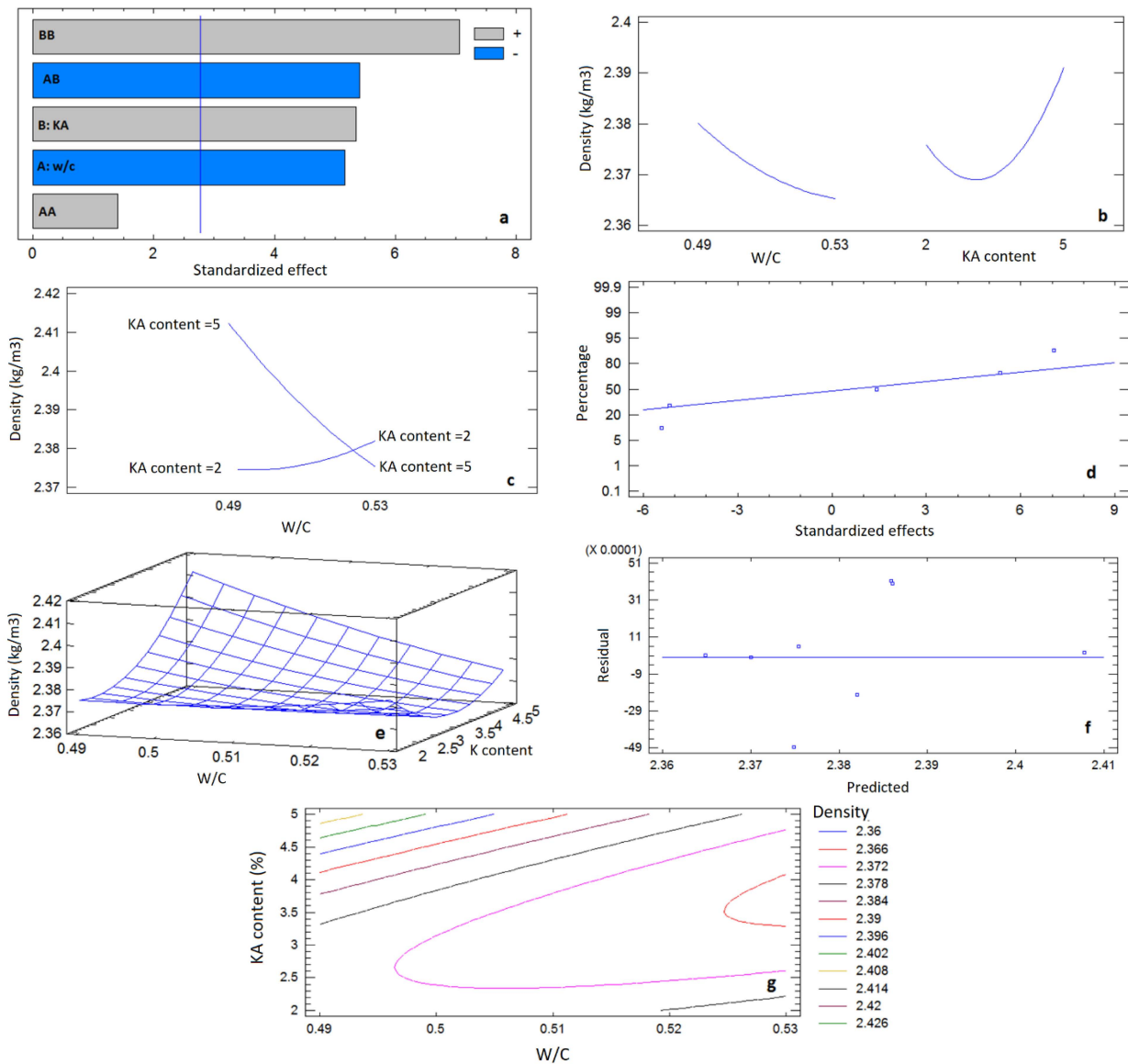


Figure 9. Plots of Pareto chart (a), main effects (b), interaction (c), normal probability (d), response surface (e), residual (f), and contour (g) for bulk density of concrete mixtures incorporated with potassium acetate (KA).

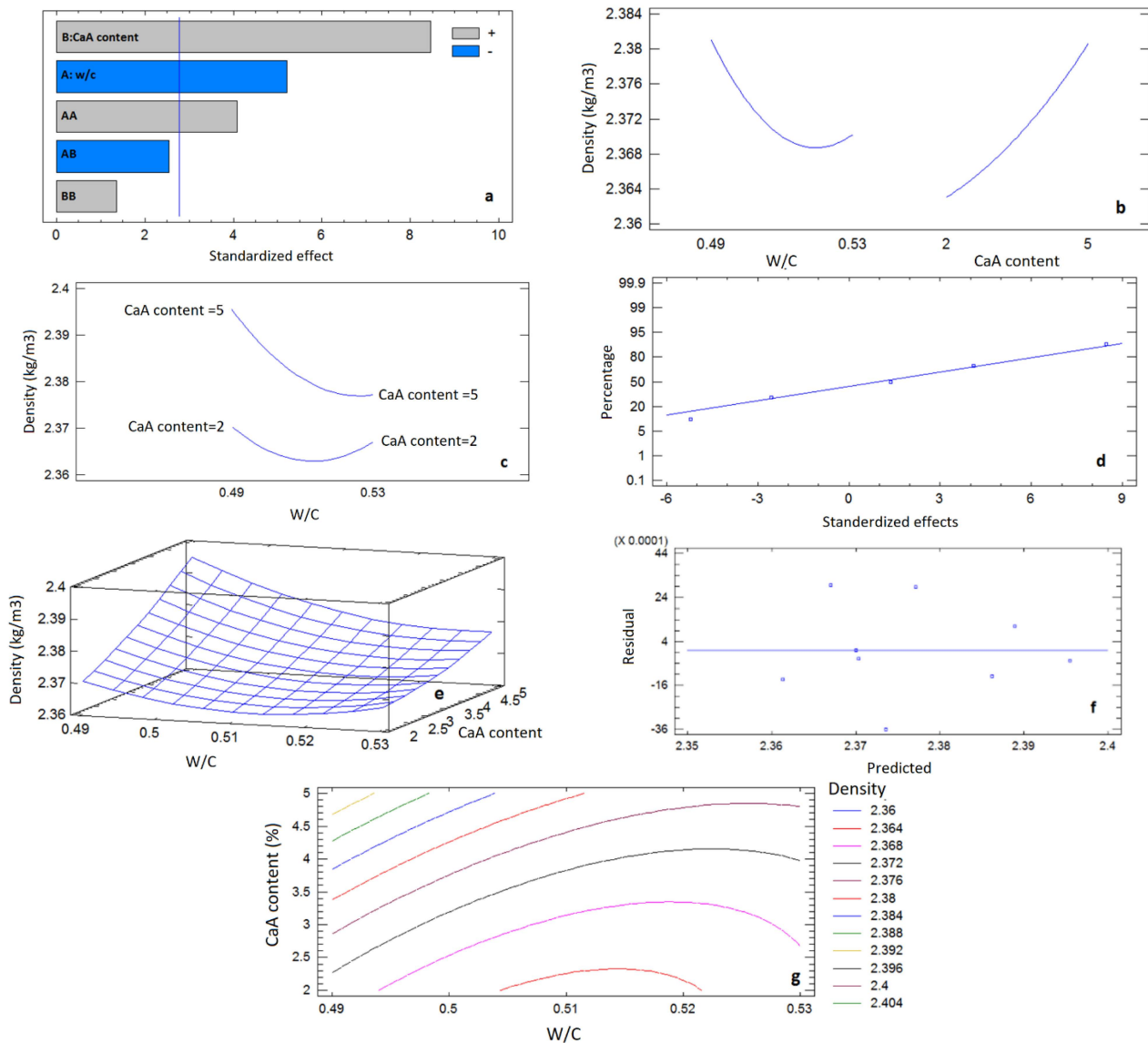


Figure 10. Plots of Pareto chart (a), main effects (b), interaction (c), normal probability (d), response surface (e), residual (f), and contour (g) for bulk density of concrete mixtures incorporated with calcium acetate (CaA).

The interaction plots reflected no remarkable interaction effects of the operating variables for density (Figures 9c, 10c and 11c). However, an interaction effect of the acetate content and w/c was observed for mixtures incorporated with KA at a higher w/c ratio (Figure 9c). The significant interactions are highlighted throughout the change in the contours to shape approximately the half ellipse and total eclipse as illustrated in (Figures 9g and 11g) representing the (2D) contour plots, respectively.

The normal probability plot presented in Figures 9d, 10d and 11d, and the plots of the residuals (Figures 9f, 10f and 11f) show the same trend established for compressive strength, which specifies the model's validity and precision describing the experimental results for bulk density.

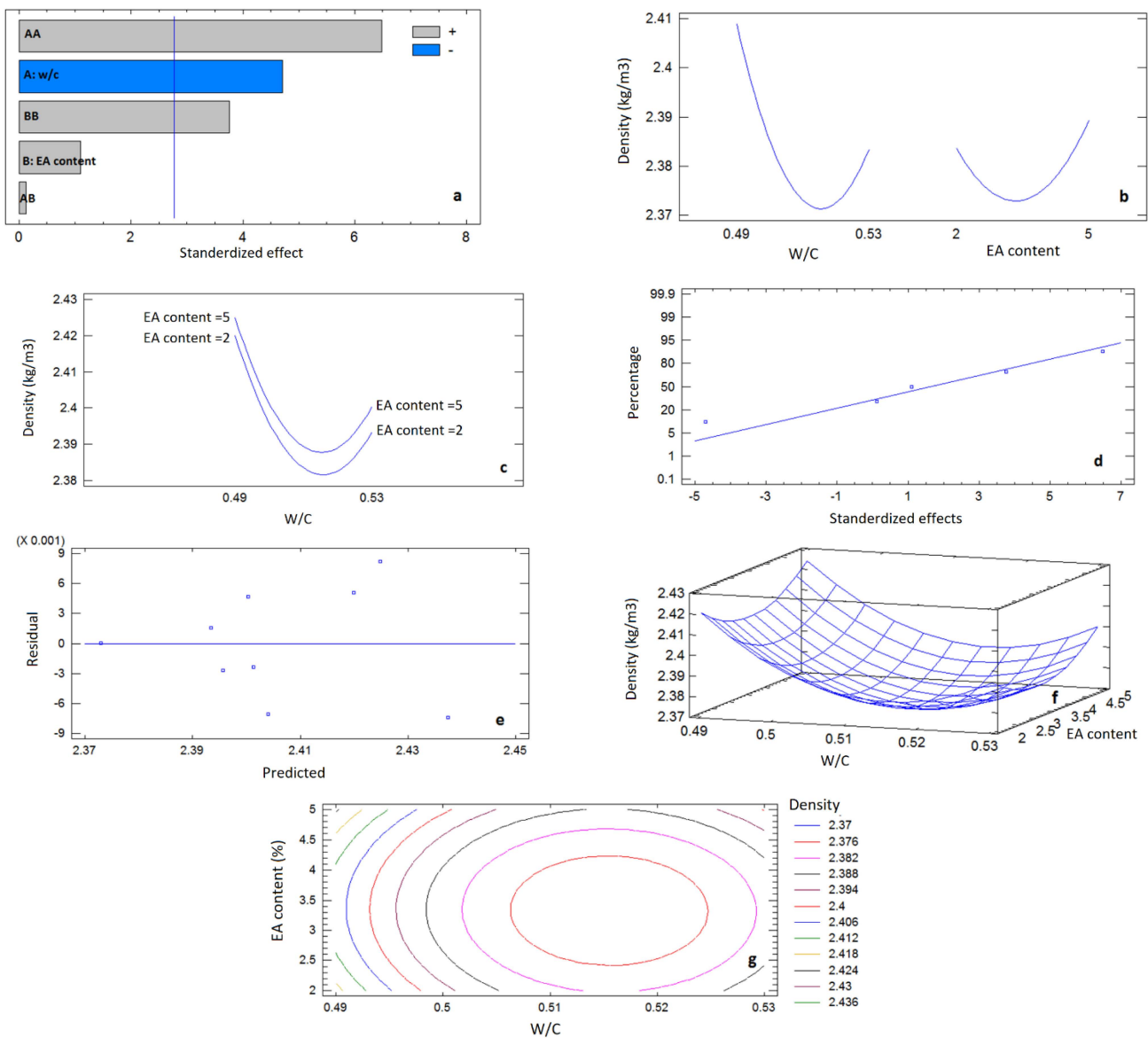


Figure 11. Plots of Pareto chart (a), main effects (b), interaction (c), normal probability (d), response surface (e), residual (f), and contour (g) for bulk density of concrete mixtures incorporated with ethyl acetate (EA).

The empirical regression model equations, regression coefficients, and the optimum bulk density values and operating variables for the mixtures formulated with different acetates are listed in Table 3. The high-regression coefficients of the estimated models confirm the model’s precision. However, less significant differences in the optimum values were estimated for bulk density compared to those estimated for compressive strength.

Table 3. The empirical regression model equations, regression coefficients, and the optimum bulk density values and operating variables for the mixtures formulated with different acetates.

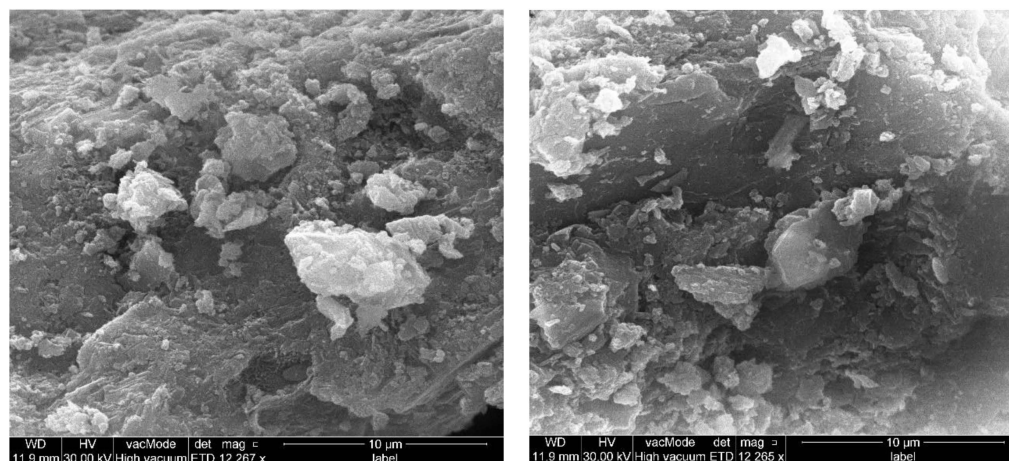
Acetate Type	The Generated Empirical Regression Model Equation	Regression Coefficient R ² (%)	Optimized Density g/cm ³	Optimized Operating Variables
Ca	Density = 5.93225 – 14.18 W + 0.064 CaA + 14.06 W ² – 0.13 W CaA + 0.0008 CaA ²	96.83	2.42	w/c = 0.48 and CaA content = 5.6 %
K	Density = 3.70748 – 5.94 W + 0.15 KA + 6.72 W ² – 0.37 W KA + 0.006 KA ²	97.17	2.45	w/c = 0.48 and KA content = 5.6%
Ethyl	Density = 17.8716 – 59.82 W – 0.048 EA + 57.97 W ² + 0.017 W EA + 0.006 EA ²	94.33	2.47	w/c = 0.48 and EA content = 5.6%

Where W = W/C, CaA = Calcium acetate content (wt.%), KA = Potassium acetate content (wt.%), EA = Ethyl acetate content (wt.%)

3.3. Microstructure Analysis

The interpretation of microstructure imaging has become well-recognized as a technique for studying the microstructure of cement and concrete composites. It is soundly established that the hydration of cement paste develops its microstructure. The hydrous cement grains form by the reaction of anhydrous cement grains with water. The products of the hydration reactions are the alite or tricalcium silicate, belite or dicalcium silicate, and calcium hydroxide. The alite and belite are accountable for the formation of the C-S-H gel. The calcium silicate hydrate is produced principally around the cement grains, while calcium hydroxide is deposited in the water-filled pores [40]. In this study, SEM images of different magnifications (the two tops are in lower magnification) were obtained for the hardened cementitious part of the control samples and acetate-modified samples. Typical SEM images for the control sample are shown in (Figure 12, top and bottom left). The figure indicates the formation of cement hydration products. Calcium hydroxide crystals are represented by areas of light gray with irregular shape, calcium silicate hydrate is signified by areas of dark gray, while the pores are displayed by black areas [41].

The top and bottom right of Figure 12 shows the typical SEM images for the hardened cementitious part of a sample incorporated with CaA. The figure illustrates less porous and denser microstructure resulting from the addition of the acetate. The denser microstructure may be owing to the high adhesion between CaA and the cement hydration products. The packed microstructure gives rise to a decrease in the volume of capillary pores in the sample incorporated with CaA. The modified microstructure enhanced by acetates enables the attainment of building materials with higher density, strength, and durability characteristics. Incorporating the acetates in the mixtures leads to reducing voids in concrete, thereby decreasing the porosity [42] and avoiding the diffusion of any fluids.

**Figure 12.** Cont.

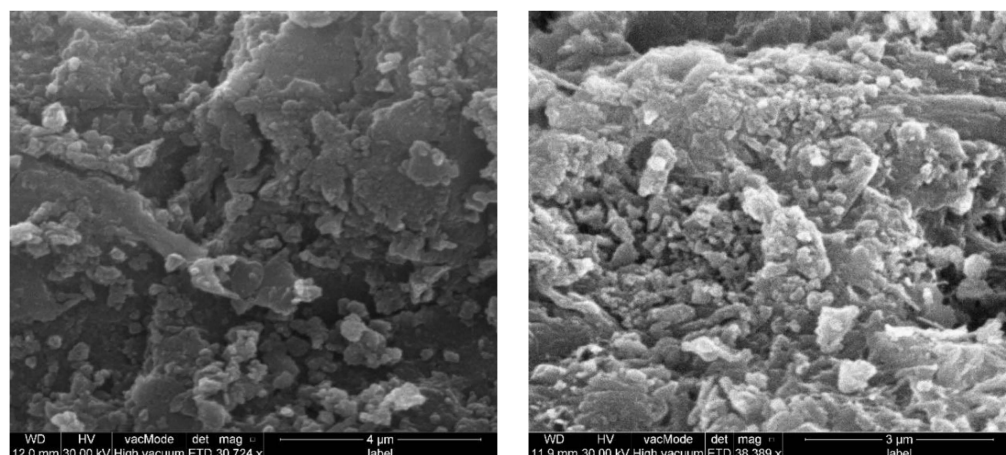


Figure 12. Hardened cementitious part of control sample (top and bottom left), sample incorporated with CaA (top and bottom right).

4. Conclusions

The effective application of chemical admixtures in concrete technology resulted in a new development in the formulation and usage of cement concrete materials. Small amounts of admixture can efficiently adjust the cement-based materials' performance. This study is a part of research aimed at examining the effect of the incorporation of potassium acetate (KA), calcium acetate (CaA), and ethyl acetate (EA) in concrete as anti-corrosion admixtures, and its impact on other concrete properties, mainly workability and compressive strength. The current work focuses on studying the impact of the merging of admixtures on the workability, density, and compressive strength of concrete based on the acetate dose and water/cement ratio. The experimental and the RSM analysis results confirmed that the relatively low-cost acetate admixtures, in particular CaA seemed promising for the manufacturing of concrete with notable workability and mechanical strength. The high rise in compressive strength linked to control mixtures was 30.8% for the mixtures incorporated with 5.6 wt.% CaA. Optimum compressive strength of 42.68, 38.76, and 38.31 MPa, and density of 2.42, 2.45, and 2.47 g/cm³ were estimated for concrete mixtures incorporated with CaA, KA, and EA, respectively using 0.48 w/c ratio. The promising results paved the way to continue the study in order to explore the impact of the admixtures on the water permeability and corrosion resistance of reinforced concrete incorporated with the optimum content of the acetate admixture, which could be used in Basrah marine construction applications.

Author Contributions: Conceptualization, A.M. and M.A.L.Y.; Methodology, A.A.A.; Software, A.A.A.; Formal analysis, A.A.A.; Investigation, A.A.A.; Resources, A.A.A.; Writing—original draft, A.A.A.; Writing—review & editing, A.M. and M.A.L.Y.; Visualization, A.A.A. All authors have read and agreed to the published version of the manuscript.

Funding: This research received no external funding.

Institutional Review Board Statement: Not applicable.

Informed Consent Statement: Not applicable.

Data Availability Statement: Not applicable.

Conflicts of Interest: The authors declare no conflict of interest.

References

1. Ibrahim, H.D.; Xue, P.; Eltahir, E.A.B. Multiple Salinity Equilibria and Resilience of Persian/Arabian Gulf Basin Salinity to Brine Discharge. *Front. Mar. Sci.* **2020**, *7*, 573. [[CrossRef](#)]
2. Dodds, W.; Goodier, C.; Christodoulou, C.; Austin, S.; Dunne, D. Corrosion risk assessment of structural concrete with coarse crushed concrete aggregate. *Proc. Inst. Civ. Eng.—Constr. Mater.* **2020**, *173*, 57–69. [[CrossRef](#)]

3. del Campo, J.M.; Negro, V. Nanomaterials in Protection of Buildings and Infrastructure Elements in Highly Aggressive Marine Environments. *Energies* **2021**, *14*, 2588. [CrossRef]
4. Bautista-Gutierrez, K.P.; Herrera-May, A.L.; Santamaría-López, J.M.; Honorato-Moreno, A.; Zamora-Castro, S.A. Recent Progress in Nanomaterials for Modern Concrete Infrastructure: Advantages and Challenges. *Materials* **2019**, *12*, 3548. [CrossRef]
5. Khudhair, N.A.; Al-Sammarraie, A.M.A. Enhancing of Corrosion Protection of Steel Rebar in Concrete Using TiO₂ Nanoparticles as Additive. *Iraqi J. Sci.* **2019**, *60*, 1898–1903. [CrossRef]
6. Amran, A.; Onaiz, A.M.; Fediuk, R.; Vatin, N.I.; Rashid, R.S.M.; Abdelgader, H.; Ozbakkaloglu, T. Self-Healing Concrete as a Prospective Construction Material: A Review. *Materials* **2022**, *15*, 3214. [CrossRef]
7. Koleva, D.A. An Innovative Approach to Control Steel Reinforcement Corrosion by Self-Healing. *Materials* **2018**, *11*, 309. [CrossRef]
8. Hossain, N.; Chowdhury, M.A.; Kchaou, M. An overview of green corrosion inhibitors for sustainable and environment friendly industrial development. *J. Adhes. Sci. Technol.* **2020**, *35*, 673–690. [CrossRef]
9. Topçu, I.B.; Eskişehir Osmangazi University; Uzunömeroğlu, A. Properties of corrosion inhibitors on reinforced concrete. *J. Struct. Eng. Appl. Mech.* **2020**, *3*, 93–109. [CrossRef]
10. Inamuddin, M.I.A.; Ahamed, M.I.; Luqman, M.; Altalhi, T. *Sustainable Corrosion Inhibitors, Ch.6*; Materials Research Forum LLC.: Millersville, PA, USA, 2019.
11. Lee, H.-S.; Saraswathy, V.; Kwon, S.-J.; Karthick, S. Corrosion Inhibitors for Reinforced Concrete: A Review. In *Corrosion Inhibitors, Principles and Recent Applications, Mahmood Aliofkhazraei*; IntechOpen: London, UK, 2017. [CrossRef]
12. Paulson, B.M.; Thomas, K.J.; Raphael, V.P.; Shaju, K.S.; Ragi, K. Mitigation of concrete reinforced steel corrosion by penta sodium triphosphate: Physicochemical and electrochemical investigations. *SN Appl. Sci.* **2020**, *2*, 1813. [CrossRef]
13. Reddy, V.S.; Prashanth, T.; Raju, S.P.; Prashanth, P. Effect of Organic and Inorganic Corrosion Inhibitors on Strength Properties of Concrete. *E3S Web Conf.* **2020**, *184*, 01112. [CrossRef]
14. Awolusi, T.; Oke, O.; Akinkulore, O.; Sojobi, A. Application of response surface methodology: Predicting and optimizing the properties of concrete containing steel fibre extracted from waste tires with limestone powder as filler. *Case Stud. Constr. Mater.* **2018**, *10*, e00212. [CrossRef]
15. Castaneda, H.; Hassan, M.; Radovic, M.; Milla, J.; Karayan, A. *Self-Healing Microcapsules as Concrete Aggregates for Corrosion Inhibition in Reinforced Concrete*; Project No. 17CLSU08; Tran-SET Publication: Baton Rouge, LA, USA, 2018.
16. Karavokyros, L.; Katsiotis, N.; Tzani, E.; Batis, G.; Sapalidis, A.; Chatzopoulos, A.; Sideris, K.; Beazi-Katsioti, M. The Effect of Mix-Design and Corrosion Inhibitors on the Durability of Concrete. *J. Mater. Sci. Chem. Eng.* **2020**, *8*, 64–77. [CrossRef]
17. Mohammed, T.U.; Ahmed, T.; Apurbo, S.M.; Mallick, T.A.; Shahriar, F.; Munim, A.; Awal, M.A. Influence of Chemical Admixtures on Fresh and Hardened Properties of Prolonged Mixed Concrete. *Adv. Mater. Sci. Eng.* **2017**, *2017*, 9187627. [CrossRef]
18. Li, D.-L.; Zheng, D.-P.; Wang, D.-M.; Zhao, J.-H.; Du, C.; Ren, C.-F. Influence of Organic Esters on Portland Cement Hydration and Hardening. *Adv. Mater. Sci. Eng.* **2018**, *2018*, 3203952. [CrossRef]
19. Mao, Q.; Zhang, J.; Ma, J.; Liu, H.; Wang, Z.; Cui, S. Improvement of Shrinkage Reduction and Superplasticity of Polycarboxylate Admixture by Ester and Silane Groups. *J. Mater. Civ. Eng.* **2022**, *34*, 10. [CrossRef]
20. Hassouna, F.M.A.; Abu-Zant, H. Effects of Superplasticizers on Fresh and Hardened Portland Cement Concrete Characteristics. *Int. J. Appl. Sci. Technol.* **2016**, *5*, 32–36. Available online: https://staff.najah.edu/media/published_research/2020/06/20/final.pdf (accessed on 9 February 2020).
21. Lai, G.; Liu, X.; Li, S.; Xu, Y.; Zheng, Y.; Guan, J.; Gao, R.; Wei, Z.; Wang, Z.; Cui, S. Development of chemical admixtures for green and environmentally friendly concrete: A review. *J. Clean. Prod.* **2023**, *389*, 136116. [CrossRef]
22. Fang, Y.; Wang, J.; Qian, X.; Wang, L.; Chen, P.; Qiao, P. A renewable admixture to enhance the performance of cement mortars through a pre-hydration method. *J. Clean. Prod.* **2022**, *332*, 130095. [CrossRef]
23. Kılınççeker, G.; Menekşe, C. The effect of acetate ions on the corrosion of reinforcing steel in chloride environments. *Prot. Met. Phys. Chem. Surfaces* **2015**, *51*, 659–666. Available online: <https://link.springer.com/article/10.1134/S2070205115040176> (accessed on 9 February 2020). [CrossRef]
24. Ryu, H.-S.; Kim, D.-M.; Shin, S.-H.; Park, W.-J.; Kwon, S.-J. Steel-Corrosion Characteristics of an Environmental Inhibitor using Limestone Sludge and Acetic Acid. *Int. J. Concr. Struct. Mater.* **2018**, *12*, 13. Available online: <https://ijcsm.springeropen.com/articles/10.1186/s40069-018-0243-x> (accessed on 9 February 2020). [CrossRef]
25. Al-Kheetan, M.J.; Rahman, M.M. Integration of Anhydrous Sodium Acetate (ASAc) into Concrete Pavement for Protection against Harmful Impact of Deicing Salt. *Prop. Interfaced Mater. Film. JOM* **2019**, *71*, 4899–4909. Available online: <https://link.springer.com/article/10.1007/s11837-019-03624-3> (accessed on 9 February 2020). [CrossRef]
26. Al-Kheetan, M.J.; Ghaffar, S.H.; Awad, S.; Chougan, M.; Byzyka, J.; Rahman, M.M. Microstructural, Mechanical and Physical Assessment of Portland Cement Concrete Pavement Modified by Sodium Acetate under Various Curing Conditions. *Infrastructures* **2021**, *6*, 113. [CrossRef]
27. Al-Kheetan, M.J.; Ghaffar, S.H.; Madyan, O.A.; Rahman, M.M. Development of low absorption and high-resistant sodium acetate concrete for severe environmental conditions. *Constr. Build. Mater.* **2020**, *230*, 117057. [CrossRef]
28. Iraqi Standard (IQ. S 5:2019) for CEM I (42.5 R). Available online: https://uowa.edu.iq/filestorage/file_1542638623.pdf (accessed on 9 February 2020).

29. Ahmed, S.M.; Kamal, I. Electrical resistivity and compressive strength of cement mortar based on green magnetite nanoparticles and wastes from steel industry. *Case Stud. Constr. Mater.* **2022**, *17*, e01712. [[CrossRef](#)]
30. Hameed, M.M.; AlOmar, M.K.; Baniya, W.J.; AlSaadi, M.A. Prediction of high-strength concrete: High-order response surface methodology modeling approach. *Eng. Comput.* **2021**, *38*, 1655–1668. [[CrossRef](#)]
31. Öztaş, A.; Pala, M.; Özbay, E.; Kanca, E.; Çağlar, N.; Bhatti, M.A. Predicting the compressive strength and slump of high strength concrete using neural network. *Constr. Build. Mater.* **2006**, *20*, 769–775. [[CrossRef](#)]
32. Silva, D.; Monteiro, P. Analysis of C3A hydration using soft X-rays transmission microscopy: Effect of EVA copolymer. *Cem. Concr. Res.* **2005**, *35*, 2026–2032. [[CrossRef](#)]
33. Silva, D.; Roman, H.; Gleize, P. Evidences of chemical interaction between EVA and hydrating Portland cement. *Cem. Concr. Res.* **2002**, *32*, 1383–1390. [[CrossRef](#)]
34. Peter, L.F.; Smith, B.C. Ionic radii for Group 1 and Group 2 halide, hydride, fluoride, oxide, sulfide, selenide and telluride crystals. *Dalton Trans.* **2010**, *39*, 7786–7791. Available online: <https://pubs.rsc.org/en/content/articlelanding/2010/dt/c0dt00401d> (accessed on 9 February 2020).
35. Cao, K.; Wang, L.; Xu, Y.; Shen, W.; Wang, H. The Hydration and Compressive Strength of Cement Mortar Prepared by Calcium Acetate Solution. *J. Adv. Civ. Eng.* **2021**, *2021*, 8817725. [[CrossRef](#)]
36. Abed, A.A.; Kamal, I.M. Factorial Design for Studying the Properties of Recycled Aggregate Concrete Exposed to Aggressive Media. *J. Eng. Res.* **2021**, *9*, 1–24. [[CrossRef](#)]
37. Abed, A.A.; Bas, Y.J.; Al-Hasani, A.; Kamal, I. Investigation on some properties of hardened cement-Biogenic ash composites. *AIP Conf. Proc.* **2022**, *2660*, 020054. [[CrossRef](#)]
38. Ma, H.; Sun, Z.; Ma, G. Research on Compressive Strength of Manufactured Sand Concrete Based on Response Surface Methodology (RSM). *Appl. Sci.* **2022**, *12*, 3506. [[CrossRef](#)]
39. Vishnupriyan, M.; Annadurai, R. A study on the macro-properties of PCB fiber-reinforced concrete from recycled electronic waste and validation of results using RSM and ANN. *Asian J. Civ. Eng.* **2023**, *24*, 1667–1680. [[CrossRef](#)]
40. Scrivener, K.L. Backscattered electron imaging of cementitious microstructures: Understanding and quantification. *Cement Concrete Compos.* **2004**, *26*, 935–945. [[CrossRef](#)]
41. Hassan, M.S. SEM-Backscattered Imaging Analysis of Cementitious Composite Matrix Incorporating Mineral Admixture. *Eng. Technol. J.* **2014**, *32*, 696–703.
42. Ozturk, A.U.; Baradan, B. Effects of admixture type and dosage on microstructural and mechanical properties of cement mortars. *KSCE J. Civ. Eng.* **2011**, *15*, 1237–1243. [[CrossRef](#)]

Disclaimer/Publisher’s Note: The statements, opinions and data contained in all publications are solely those of the individual author(s) and contributor(s) and not of MDPI and/or the editor(s). MDPI and/or the editor(s) disclaim responsibility for any injury to people or property resulting from any ideas, methods, instructions or products referred to in the content.